THE JOURNAL OF PHYSICAL CHEMISTRY C LETTERS

2007, *111,* 14621−14624
Published on Web 09/19/2007

Electrochemical Deposition of Chromium Core−Shell Nanostructures on H−Si(100): Evolution of Spherical Nanoparticles to Uniform Thin Film without and with Atop Hexagonal Microrods

L. Y. Zhao, A. C. Siu, L. J. Pariag, Z. H. He, and K. T. Leung*

WATLab, and Department of Chemistry, University of Waterloo, Waterloo, Ontario N2L 3G1, Canada

Received: July 23, 2007; In Final Form: September 3, 2007

Electrodeposition in Cr(VI) and Cr(III) aqueous electrolytes is found to produce, respectively, granular and spherical core−shell nanoparticles on H-terminated Si(100). For the granular nanoparticles obtained by electrodeposition in CrO_3 and H_2SO_4 electrolyte solution, both the morphology and number density remain discernibly similar while the particle size increases with increasing charge transfer. In the $CrCl_3$ electrolyte, evolution of the spherical nanoparticles to homogeneous Cr films without and with atop hexagonal microrods with increasing charge transfer is observed. The viability of producing a homogeneous Cr film on the Si substrate is therefore demonstrated. Both the granular Cr nanoparticles and the Cr film consist of predominantly Cr metallic core and Cr_2O_3 outer shell covered by surface CrO_3, while the novel hexagonal microrods are made up of a metallic Cr core and a CrOOH shell.

1. Introduction

The metallization of Si has attracted a lot of attention because the dimensions of the device have reached the submicrometer level. For metals such as gold and iron, poor adhesion to Si is found. Because a chromium film exhibits good adhesion to Si, it is often used as an adhesion layer in order to provide good ohmic contact with metallic conductors. Furthermore, the formation of metal silicide is undesirable in device fabrication, and a diffusion barrier, specifically a Cr layer, is commonly used to prevent such formation.[1,2] The method of choice used to produce a Cr film on a Si substrate involves sputter-deposition. Although a great deal of work involving electroplating of Cr films on a variety of substrates is available in the literature,[3] only one recent work involving Cr electrodeposition on Si has been reported. In particular, Georgescu et al. obtained "ultrathin films" of nanocrystalline Cr on a H−Si(100) (i.e., H-terminated) substrate by electrodeposition in an aqueous CrO_3 solution.[4] Separate fine particles were obtained at a charge density less than 200 C cm^{-2}, and increasing the charge density increased both the size and density of the Cr nanocrystalline islands. However, this work provides strong evidence for nanoparticles (NPs) of 2−150 nm in size distributed over the Si substrate and no direct data for a continuous film is reported. Following the earlier work of decorative and hard chromium electroplating that employed exclusively CrO_3 as the electrolyte, we also attempt to synthesize a uniform Cr film on Si by using the same rather toxic hexavalent Cr electrolyte solution. Like Georgescu et al.,[4] we only observe discrete NPs, granular in shape and considerably larger in size (360 nm to 2.2 μm at a charge density of 0.012−6.0 C cm^{-2}) than those reported previously. By switching to a trivalent Cr electrolyte solution ($CrCl_3$) that is much safer to handle but has never previously been used for Cr electrodeposition, we produce a continuous Cr film on a H−Si(100) substrate for the first time by electrochemical methods. Furthermore, by manipulating the charge transfer during the electrodeposition, we can also obtain spherical NPs (7−40 nm) and unique hexagonal microrods at low and high charge transfers, respectively.

2. Experimental Details

All of the electrodeposition experiments were performed in a three-electrode cell with a potentio/galvanostat electrochemical workstation described elsewhere.[5] Briefly, the working electrodes were single-side-polished rectangular (15 × 2.5 mm^2) Si(100) chips (0.4 mm thick, p-type with a resistivity of 1.0−1.5 mΩ·cm), which have been H-terminated by a standard procedure.[6] The Si substrate was inserted into a clamp holder and securely fastened and then placed into the electrochemical cell holder with 40% of the chip immersed inside the electrolyte solution. Chromium deposits on the H−Si(100) substrate were obtained by amperometry potentiostatically in two different deoxygenated electrolyte solutions of 6 mM CrO_3 and 10 mM H_2SO_4 (pH = 2.1) and of 0.1−10 mM $CrCl_3$ and 0.1 M $NaClO_4$ (pH = 5.4−3.1). Although it is difficult to monitor any pH change in real time during the electrodeposition in our present setup, only negligible change in the pH before and after the electrodeposition is observed because of the minute amount of materials consumed in the deposition. Because $CrCl_3$ solution is a very strong reducing agent and oxidized easily in air, a fresh $CrCl_3$ solution must be prepared before each electrodeposition. After the deposition, the Si substrate was removed from the cell, thoroughly rinsed with Millipore water, and dried in N_2. The morphology and chemical-state composition of the resulting electrodeposits were further characterized by using field-emission scanning electron microscopy (SEM), atomic force microscopy (AFM), and X-ray photoelectron spectroscopy

* Corresponding author. E-mail: tong@uwaterloo.ca.

10.1021/jp0757762 CCC: $37.00

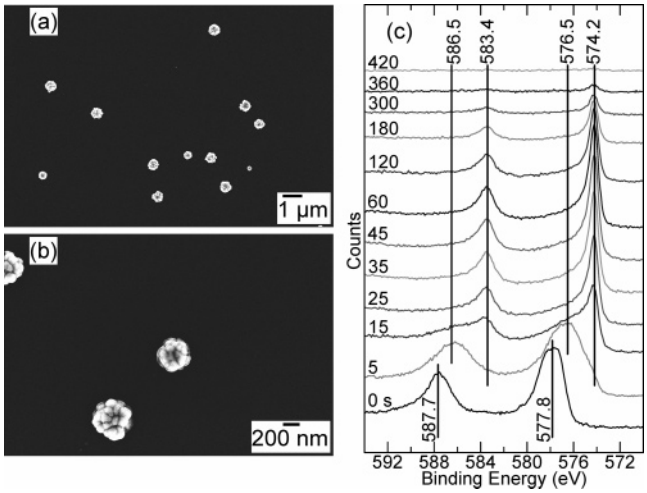

Figure 1. (a and b) SEM images and (c) the corresponding Cr 2p XPS spectra collected as a function of sputtering time (in seconds) of granular Cr nanoparticles electrodeposited on H−Si(100) at −1.4 V and 0.012 C cm^{-2} in an aqueous solution of 6 mM CrO_3 and 10 mM H_2SO_4.

(XPS) as a function of sputtering depth (depth-profiling), respectively.

3. Results and Discussion

The electrodeposition on H−Si(100) substrate was performed in an aqueous solution of 6 mM CrO_3 and 10 mM H_2SO_4 for 1 s at −1.2 V and −1.4 V (relative to the Ag/AgCl reference electrode), respectively. At −1.2 V, no Cr deposition is detected on the Si substrate by SEM (not shown). At −1.4 V, granular NPs (with an average diameter of 360 nm) were obtained at a charge density of 0.012 C cm^{-2} and shown in Figure 1. Increasing the deposition time to 100 s, and hence correspondingly the charge density to 6.0 C cm^{-2}, appears to increase the particle size to 2.2 μm, with no apparent change in the number density. Except for the larger particle size, our present result is therefore similar to that of Georgescu et al.,[4] in which no continuous Cr film was produced on the Si substrate by using this hexavalent electrolyte. Both the granular shape and the low number density of the Cr NPs indicate that the number of the nucleation sites on the H−Si(100) during electrodeposition is very low. The corresponding XPS depth profiling spectra of these Cr electrodeposits are shown in Figure 1c. Before sputtering, the as-deposited NPs exhibit a Cr $2p_{3/2}$ ($2p_{1/2}$) feature at 577.8 eV (587.7 eV) corresponding to $Cr(OH)_3$.[7] After the initial sputtering of 5 s, the broad Cr $2p_{3/2}$ ($2p_{1/2}$) feature at 576.5 eV (586.5 eV) is observed and can be assigned to Cr_2O_3,[8] which makes up the shell of the NPs. Upon further sputtering, a sharp Cr $2p_{3/2}$ ($2p_{1/2}$) feature appears to emerge at 574.2 eV (583.4 eV) and it can be attributed to a predominant metallic Cr core.[9] The granular Cr NPs therefore consist of individual predominant metallic Cr cores, with Cr_2O_3 shells covered by surface $Cr(OH)_3$. It should be noted that the occurrence of the metallic Cr core is not the result of sputtering because it has been reported that sputtering cannot cause reduction of chromium oxide.[10]

To produce a Cr film on H−Si(100), we repeated the above electrodeposition experiment with a trivalent Cr electrolyte. Figure 2a shows a typical current transient curve for Cr electrodeposition in a solution of 0.1 mM $CrCl_3$ and 0.1 M $NaClO_4$ at −1.3 V. The current transient is found to increase sharply due to the nucleation and growth of individual nuclei. After reaching a maximum, the current then starts to decrease

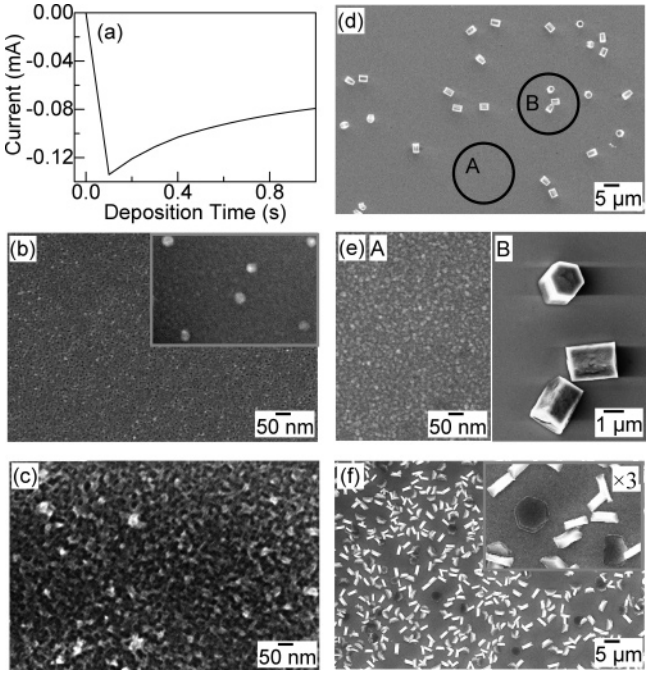

Figure 2. (a) Current−time curve for Cr electrodeposition on a H−Si(100) at −1.3 V in an aqueous solution of 0.1 mM $CrCl_3$ and 0.1 M $NaClO_4$, and SEM images of (b) Cr nanoparticles obtained at 1 mC cm^{-2} charge density; (c) Cr film at 50 mC cm^{-2}; (d and e) hexagonal microrods on the top of the Cr film at 100 mC cm^{-2}. The Cr nanoparticles shown as an inset in b and hexagonal microrods shown in f are electrodeposited on H−Si(100) at −1.3 V, respectively, at 20 mC cm^{-2} and 600 mC cm^{-2} charge density in 10 mM $CrCl_3$ and 0.1 M $NaClO_4$. A magnified view of the latter is also shown as an inset in f.

gradually as the diffusion zones of the growing number of individual nuclei overlap.[11] To study the effect of charge transfer, we performed the electrodeposition at three charge densities (1, 50, and 100 mC cm^{-2}). Evidently, at a low charge density of 1 mC cm^{-2}, spherical NPs with an average diameter of 7 nm are obtained on the Si substrate (Figure 2b). The Cr NPs of 40-nm diameter shown as an inset in Figure 2b are obtained by electrodeposition on H−Si(100) at −1.3 V and 20 mC cm^{-2} in a 10 mM $CrCl_3$ and 0.1 M $NaClO_4$ solution. Previous studies have reported the synthesis of metallic Cr NPs of different particle sizes by a variety of methods, including hydrogen plasma-metal reaction (100 nm),[12] ball-milling (~20 nm),[13] arc-discharge (10−50 nm),[14] reduction of $CrCl_2$ with either $LiBH_4$ or $NaBH_4$ (5 nm),[15] thermolysis of a chromium Fisher carbine complex (2.5−6.0 nm),[16] gas evaporation (2−79 nm),[17−21] and dip-coating with posttreatments (2−30 nm).[22] The present work therefore provides a new method of producing monodispersed Cr NPs (3−10 nm) by electrochemical deposition on H−Si(100) substrates, and may be of interest to studying the unique magnetic properties of these near-quantum-sized Cr NPs.[15,18] When the charge density is increased to 50 mC cm^{-2}, we observe a continuous Cr film (Figure 2c) with an approximate film thickness of 15 nm and rms roughness of 2.7 nm as estimated by AFM. As expected, further increase in the charge density produces a thicker and smoother film, and upon reaching a critical charge density (80 mC cm^{-2}), a few highly dispersed rod-shaped NPs emerge suddenly on top of the smooth film. Further increase of the charge density to 100 mC cm^{-2} appears to produce hexagonal microrods on top of the Cr film (Figure 2d). At a higher magnification, SEM reveals a smoother film (Figure 2e, A) with a rms roughness of 2.0 nm and a larger film thickness of 22 nm (both estimated by

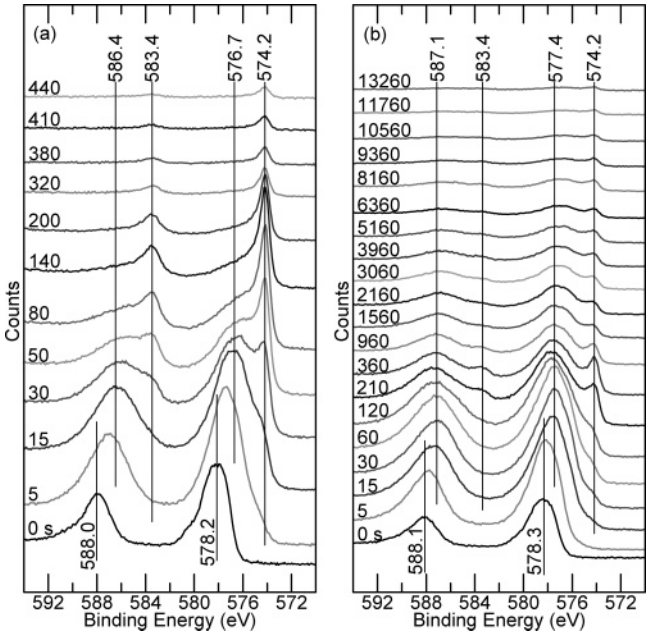

Figure 3. Cr 2p XPS spectra collected as a function of sputtering time (in seconds) for Cr film (a) without and (b) with atop hexagonal microrods electrodeposited on a H−Si(100) at −1.3 V in aqueous solutions of 0.1 mM $CrCl_3$ and 0.1 M $NaClO_4$ at 50 mC cm^{-2} and of 10 mM $CrCl_3$ and 0.1 M $NaClO_4$ at 600 mC cm^{-2}, respectively.

AFM), in comparison with that obtained at 50 mC cm^{-2} (Figure 2c). The average diameter and length of the hexagonal microrods are found to be 1.6 and 2.4 μm, respectively (Figure 2e, B). Furthermore, the number density, size and diameter-to-length aspect ratio of the hexagonal microrods can be varied by changing the $CrCl_3$ concentration and charge density. At a lower $CrCl_3$ concentration (0.1 mM), the microrods appear shorter and sparsely dispersed (Figure 2d), whereas at a higher concentration (10 mM) they appear longer and more densely populated (Figure 2f). Differences in the diameter-to-length aspect ratio are also observed between the microrods obtained at 0.1 mM (1.6 μm: 2.4 μm) and 10 mM $CrCl_3$ concentrations (800 nm:3.0 μm). At an even higher charge density exceeding 1 C cm^{-2} in a 10 mM $CrCl_3$ solution, the microrods appear to be broken with distorted shapes and to cluster together (not shown). The mechanism of the shape evolution of these hexagonal microrods remains unclear. In separate experiments, we also qualitatively evaluate the adhesion of the Cr films without the hexagonal microrods by performing a standard Scotch-tape stick-and-peel test. These tests show that the Cr films could not be peeled off by removing the tape and indicate that the adhesion of the Cr films on the Si substrate is strong.

The corresponding Cr 2p XPS spectra obtained as a function of sputtering depth have also been obtained for the Cr spherical NPs (Figure 2b) and the Cr film (Figure 2c). Because the depth-profiling spectra for both samples appear to be similar (with the exception of the absolute intensity), we only show in Figure 3a the XPS depth-profiling spectra of the Cr film. For the as-deposited Cr film, the Cr $2p_{3/2}$ ($2p_{1/2}$) feature found at 578.2 eV (588.0 eV) can be attributed to CrO_3, in good accord with the literature values.[9,23] After sputtering for 15 s, the two new Cr $2p_{3/2}$ ($2p_{1/2}$) features emerged at 576.7 eV (586.4 eV) and 574.2 eV (583.4 eV) could be assigned to Cr_2O_3 and metallic Cr, respectively. Further sputtering appears to reduce the Cr_2O_3 features first and then the metallic Cr feature, consistent with the model that the Cr film (spherical NP) consists of a metallic Cr core and a Cr_2O_3 shell covered by surface CrO_3. The XPS depth-profiling spectra for the Cr film with atop hexagonal Cr microrods (Figure 2f) are shown in Figure 3b. Before sputtering, the as-deposited sample exhibits similar Cr $2p_{3/2}$ ($2p_{1/2}$) feature at 578.3 eV (588.1 eV) corresponding to CrO_3. Sputtering the sample for 60 s appears to produce a Cr $2p_{3/2}$ ($2p_{1/2}$) feature at 577.4 eV (587.1 eV), which is in good accord with the literature value for CrOOH.[24] Further sputtering the sample for 210 s clearly exposes the well-defined sharp Cr $2p_{3/2}$ ($2p_{1/2}$) feature at 574.2 eV (583.4 eV) of metallic Cr. Both the CrOOH and metallic Cr features are reduced concurrently until complete removal upon further sputtering. Given that the CrOOH does not appear on the Cr film without the hexagonal microrods (Figure 3a), CrOOH observed on the present sample (Figure 3b) likely resides only on the microrods, forming the outside shell covering the metallic Cr core inside.

It should be noted that our choice of using H_2SO_4 in the Cr(VI) electrolyte is based on what is commonly used in Cr electroplating in the industry, where H_2SO_4 works as a catalyst for the electrodeposition.[25−27] For electrodeposition in the Cr(III) electrolyte, $NaClO_4$ is commonly used as a supporting electrolyte. When 0.1 M $NaClO_4$ (instead of H_2SO_4) is used in the 6 mM CrO_3 solution, electrodeposition under similar conditions (i.e., −1.4 V and 1 s) does not produce any Cr deposit. This is not surprising because of the absence of the H_2SO_4 catalyst for electrodeposition in CrO_3. Alternatively, when 10 mM H_2SO_4 (instead of $NaClO_4$) is used in the 10 mM $CrCl_3$ solution, spherical nanoparticles are observed at −1.3 V and charge density of 600 mC cm^{-2}. In contrast, in the present case when the electrodeposition is performed in a 10 mM $CrCl_3$ solution mixed with 0.1 M $NaClO_4$, hexagonal microrods atop of a Cr film are observed under the same deposition conditions. The difference could be due to the different current efficiencies of and different types and amounts of nucleation sites available to the different electrolytes employed.

In the present work, electrodeposition in the Cr(VI) electrolyte at −1.4 V and with a charge density of 6.0 C cm^{-2} could only produce granular shaped Cr NPs with a low number density. In the recent work reported by Georgescu et al.,[4] "spatially scattered fine particles" were observed at a charge density as high as 204.0 C cm^{-2}. The present work therefore confirms the finding of Georgescu et al.,[4] with our similar observation of granular NPs without a continuous film at a lower charge density. Furthermore, given that (1) the deposition potentials employed are very similar in both Cr(VI) and Cr(III) electrolytes and (2) a continuous Cr film has already been prepared successfully in the Cr(III) electrolyte with a much lower charge density of 50 mC cm^{-2} at −1.3 V (and not in the Cr(VI) electrolyte), it is therefore not necessary to perform electrodeposition in the Cr(VI) electrolyte at a higher charge density. It is also not necessary to perform further electrodeposition at a more negative potential than −1.4 V because a higher percentage of the charge is expected to be consumed by the hydrogen evolution reaction at a more negative potential. In contrast to the work of Georgescu et al.,[4] the present work provides a new method of preparing a continuous Cr film by electrodeposition in a Cr(III) electrolyte.

The number of nucleation sites on the substrate may greatly depend on the nature of the electrolyte solution involved in the electrodeposition. For electrodeposition in the hexavalent electrolyte, the presence of only granular NPs suggests that the number of nucleation sites is low, which correspondingly leads to a slow growth rate. In the case of electrodeposition in a trivalent electrolyte, the number of nucleation sites appears to increase significantly, thereby increasing the number density

of the NPs, which eventually leads to the formation of a continuous Cr film.

4. Concluding Remarks

Electrodeposition is found to be a viable alternative to vacuum evaporation techniques for depositing a homogeneous Cr film on the Si substrate. Electrodeposition in a CrO_3 and H_2SO_4 solution is found to produce granular NPs consisting predominantly of metallic Cr cores, with Cr_2O_3 shells covered by surface $Cr(OH)_3$. Instead of using the toxic Cr(VI) electrolyte, a safer Cr(III) solution ($CrCl_3$ and $NaClO_4$) is used in the present electrodeposition procedure. Three different morphologies of Cr electrodeposits, including spherical Cr NPs, Cr film without and with hexagonal shaped Cr microrods on top, are obtained with increasing charge density. XPS depth-profiling experiments show that both the spherical Cr NPs and the Cr film consist of Cr metallic inner core and Cr_2O_3 outer shell covered by surface CrO_3. The novel hexagonal microrods are found to consist of a metallic Cr core and a CrOOH shell that is believed to give its unique hexagonal shape.

Acknowledgment. This work is supported by the Natural Sciences and Engineering Research Council of Canada.

References and Notes

(1) Ezer, Y.; Härkönen, J.; Arpiainen, S.; Sokolov, V.; Kuivalainen, P.; Saarilahti, J.; Kaitila, J. *Phys. Scr.* **1999**, *T79*, 228.

(2) Chuang, J. C.; Tu, S. L.; Chen, M. C. *J. Electrochem. Soc.* **1999**, *146*, 2643.

(3) Schlesinger, M.; Paunovic, M. *Modern Electroplating*, 4th ed.; Wiley, New York, 2000; p 289.

(4) Georgescu, V.; Sîrbu, C.; Apetroaiei, N. *J. Optoelectron. Adv. Mater.* **2006**, *8*, 1456.

(5) Zhao, L. Y.; Eldridge, K. R.; Sukhija, K.; Jalili, H.; Heinig, N. F.; Leung, K. T. *Appl. Phys. Lett.* **2006**, *88*, 033111.

(6) *Handbook of Semiconductor Wafer Cleaning Technology*; Kern, W., Ed.; Noyes: Park Ridge, NJ, 1993.

(7) Biesinger, M. C.; Brown, C.; Mycroft, J. R.; Davidson, R. D.; McIntyre, N. S. *Surf. Interface Anal.* **2004**, *36*, 1550.

(8) Aronniemi, M.; Sainio, J.; Lahtinen, J. *Surf. Sci.* **2005**, *578*, 108.

(9) Moulder, J. F.; Stickle, W. F.; Sobol, P. E.; Bomben, K. D. *Handbook of X-ray Photoelectron Spectroscopy*, 2nd ed.; J. Chastain, Ed.; Perkin-Elmer Corp.: Eden-Prairie, MN, 1992.

(10) Carta, G.; Natali, M.; Rossetto, G.; Zanella, P.; Salmaso, G.; Restello, S.; Rigato, V.; Kaciulis, S.; Mezzi, A. *Chem. Vap. Deposition* **2005**, *11*, 375.

(11) Radisic, A.; Long, J. G.; Hoffmann, P. M.; Searson, P. C. *J. Electrochem. Soc.* **2001**, *148*, C41.

(12) Ishibashi, H.; Nakahigashi, K.; Tsunoda, Y. *J. Phys.: Condens. Matter* **1993**, *5*, L415.

(13) Abdul-Razzaq, W.; Seehra, M. S. *Phys. Status Solidi A* **2002**, *193*, 94.

(14) Zhang, W. S.; Brück, E.; Zhang, Z. D.; Tegus, O.; Li, W. F.; Si, P. Z.; Geng, D. Y.; Buschow, K. H. *J. Physica B* **2005**, *358*, 332.

(15) Green, M.; O'Brien, P. *Chem. Commun.* **2001**, 1912.

(16) Son, S. U.; Jang, Y. J.; Yoon, K. Y.; An, C. H.; Hwang, Y.; Park, J. G.; Noh, H. J.; Kim, J. Y.; Park, J. H.; Hyeon, T. *Chem. Commun.* **2005**, 86.

(17) Matsuo, S.; Nishida, I. *J. Phys. Soc. Jpn.* **1980**, *49*, 1005.

(18) Tsunoda, Y.; Nakano, H.; Matsuo, S. *J. Phys.: Condens. Matter* **1993**, *5*, L29.

(19) Furubayashi, T.; Nakatani, I. *J. Appl. Phys.* **1993**, *73*, 6412.

(20) Fitzsimmons, M. R.; Eastman, J. A.; Robinson, R. A.; Lawson, A. C.; Thompson, J. D.; Movshovich, R.; Satti, J. *Phys. Rev. B* **1993**, *48*, 8245.

(21) Fitzsimmons, M. R.; Eastman, J. A.; Von Dreele, R. B.; Thompson, L. J. *Phys. Rev. B* **1994**, *50*, 5600.

(22) Tilley, R. D.; Jefferson, D. A. *J. Mater. Chem.* **2002**, *12*, 3809.

(23) Kunst, M.; Jaegermann, W.; Schmeisser, D. *Appl. Phys. A* **1987**, *42*, 57.

(24) Krawiec, H.; Vignal, V.; Heintz, O.; Oltra, R.; Chauveau, E. *Metall. Mater. Trans. A* **2006**, *37*, 1541.

(25) Leisner, P.; bech-nielsen, G.; Møller, P. *J. Appl. Electrochem.* **1993**, *23*, 1232.

(26) Joshi, A.; Kulkarni, S. K. *J. Mater. Sci.* **1990**, *25*, 1357.

(27) McCormick, M.; Dobson, S. J. *J. Appl. Electrochem.* **1987**, *17*, 303.